ORGANOMETALLICS

Article

pubs.acs.org/Organometallics

Gold(I) Complexes Derived from Alkynyloxy-Substituted Anthraquinones: Syntheses, Luminescence, Preliminary Cytotoxicity, and Cell Imaging Studies

Rebeca G. Balasingham,[†] Catrin F. Williams,[‡] Huw J. Mottram,[§] Michael P. Coogan,*[,†] and Simon J. A. Pope*[,†]

[†]School of Chemistry, Cardiff University, Main Building, Cardiff CF10 3AT, Cymru/Wales

[‡]School of Biosciences, Cardiff University, Main Building, Cardiff CF10 3AT, Cymru/Wales

[§]School of Pharmacy, Cardiff University, Redwood Building, Cardiff CF10 3NB, Cymru/Wales

Supporting Information

ABSTRACT: A series of mono- and dimetallic Au(I) triphenylphosphine complexes derived from 1,2-, 1,4-, and 1,8-dialkynyloxyanthraquinone have been prepared. The photophysical and cytotoxic behavior of the ligands and complexes have been explored, with all of the complexes showing both appreciable cytotoxicity against the MCF-7 carcinoma cell line and useful room-temperature anthraquinone-based visible luminescence, which allowed their successful application as fluorophores in cell imaging microscopy. The implications of the photophysical and toxicological properties for the design and investigation of gold-based anticancer agents are discussed.

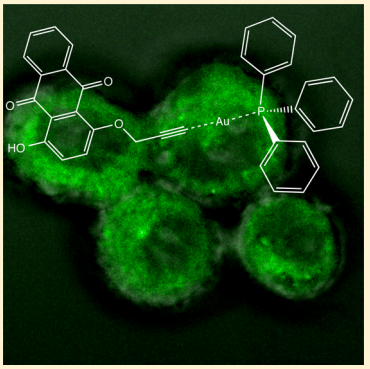

INTRODUCTION

The therapeutic potential of gold(I) complexes has been demonstrated in many studies, and there are a number of gold(I) species that have been applied in therapy, notably "auranofin", an antiarthritic that has recently shown promise in other areas, including anti-HIV.[1] In fact, "chrysotherapy" has a centuries-old tradition, but it is only very recently that, in line with the rise of applications of organometallic species in biology and medicine, there has been interest in the applications of organogold species. In fact, a small range of cyclometalated Au(III)-η^1 aryl complexes derived from dimethylbenzylamine[2] showed early promise in the 1990s, but then the area was largely dormant until much more recently. In 2006 the first reports appeared of Au(I) NHC complexes as potential antitumor agents,[3] and in 2009 a study[4] of the cytotoxicity of Au(I) alkynyls was reported. These reports followed from recent investigations of the cytotoxicity of Au(I) thiolate and phosphine complexes, which have indicated a mode of action involving interference with mitochondria, triggering release of cytochrome *c*, and inducing apoptosis.[5] While the mode of action is not fully understood, it may involve binding of gold ions to selenocysteine residues of thioredoxin reductase (Trx-R), in line with the high affinity of gold for selenium donors.[6] It is interesting, however, that a cell imaging study with one of the Au(I)NHC complexes[3] designed to target mitochondria, which had been reengineered for luminescence, showed not mitochondrial localization, but entrainment in lysosomes.[7] Recent studies on a gold complex incorporating a tethered luminescent naphthalimide chromophore have shown DNA intercalation and anticancer activity:[8] the complexes demonstrate a general enhancement in activity compared to [Cl-Au-(PEt_3)], probably due to improved uptake by nuclei.

However, a study of a range of Au(I) alkynyls that showed moderate to high cytotoxicity also studied cellular distribution by fluorescence imaging, showing that the complex was distributed throughout the cells, rather than being limited to one area.[9] These last two reports combine the potential therapeutic properties of gold complexes with another well-known property of certain gold complexes, their luminescence. There are a wide range of mechanisms by which gold complexes can show luminescence, including gold−gold interactions in either the solid state or multinuclear systems[10] and in particular many interesting phenomena associated with phosphorescence from gold(I) alkynyls, which have been widely investigated.[11] Given their apparent apoptosis induction and potentially useful luminescence, applications of Au(I) alkynyls in combined studies aimed at using fluorescent cell imaging to inform cytotoxicity studies became attractive, particularly if these properties can be coupled with a vector of known biological utility, as a starting point for their design.

Special Issue: Organometallics in Biology and Medicine

Received: May 30, 2012
Published: August 3, 2012

The biological and pharmaceutical science of anthraquinones has received significant attention, with derivatives showing a breadth of applicability (e.g., antibiotics and antitumor activity):[12] the hydroxy-anthraquinone unit has been identified as a key biologically active site in antitumor anthracyclines.[13] Hydroxy-anthraquinone is a naturally occurring genotoxic compound found in medicinal plants, including *Rubia tinctorium* L.;[13b,c] its increased commercialization exploits an antimicrobial effect.[13a] The antitumor activity of anthraquinones is thought to be due to the intercalation of the planar ring system between the base pairs of the DNA,[13c] resulting in an inhibition of DNA transcription and replication.[13c] The extraction from *Scutia myrtina* has yielded three anthrone-anthraquinone derivatives, a new bisanthrone-anthraquinone, and the known aloesaponairn I,[14] which displayed antiproliferative (cancer/antiangiogenic) and moderate antimalarial activities. Rhubarb root contains the natural anthraquinones aloe-emodin, chrysophanol, physicon, and rhein,[15] derivatives that are based on a 1,8-dihydroxyanthraquinone core: studies have shown that different substitution patterns can affect the antiangiogenic activity of a given anthraquinone.

In an optical context, our previous studies have shown that picolyl-functionalized anthraquinone chromophores (L) can be incorporated into luminescent complexes based on *fac*-$[Re(CO)_3(bpy)(L)]^+$, giving species that are generally dual emissive from both anthraquinone-centered (actually charge transfer dominated) and ^{3}MLCT excited states.[16] Amido-functionalized anthraquinone chromophores can also be utilized as chromophoric antennae for near-IR emitting lanthanide complexes,[17] advantageously facilitating visible light sensitization. Such species have also been shown to bind to DNA, with the affinity being determined by the substitution pattern of the anthraquinone (1,4- vs 1,5-diamido).[18]

The dual advantages offered by the optical and biological functionality of anthraquinone units have led to their limited use in imaging studies. The ability of anthraquinone-tethered platinum(II) complexes to intercalate with DNA[19a] has led to enhanced cellular accumulation in cancer cell (model) spheroids[19b] when compared to cisplatin. Uptake was tracked within the spheroid, via the fluorescent anthraquinone moiety, using confocal microscopy.

Therefore, the aims of this study were to investigate the potential application of gold(I) alkynyls derived from hydroxy-substituted anthraquinone fluorophores, with a view to exploiting the biological properties and photophysical characteristics of the respective component parts.

RESULTS AND DISCUSSION

Synthesis of Ligands. Anthraquinone-derived ligands $\mathbf{L}^{1-7}$ were synthesized by the base-mediated reaction of the relevant hydroxyanthraquinone with propargyl bromine (Figure 1). Both the reaction time and the base used had an influence on the nature and yield of the products formed. Literature reports the use of potassium carbonate as the base,[20] and this was successful for the 1,2-dipropargyl species, $\mathbf{L}^1$, which was formed in moderate (30−40%) yield as a single product. However, this route was less successful for the ligands derived from the 1,4- and 1,8-dihydroxyanthraquinone isomers $\mathbf{L}^2$, $\mathbf{L}^3$, $\mathbf{L}^6$, and $\mathbf{L}^7$, which required the improved solubility of sodium carbonate to give reasonable yields. The situation was more complex in the specific cases of the dialkynes: although $\mathbf{L}^1$ was formed in reasonable yield (30−40%) as a single product with two propargyl units appended to the core, attempts to generate $\mathbf{L}^3$ and $\mathbf{L}^7$ under the same conditions produced a mixture of mono- (i.e., $\mathbf{L}^2$ and $\mathbf{L}^6$) and dipropargylated products (using either sodium or potassium carbonate), which were each isolated in poor yields. Increasing the reaction time by an additional 48 h (from a standard 72 h for previous examples) resulted in a 5-fold increase in yield for the dialkynyl species ($\mathbf{L}^3$ 3 days 5.6%, 5 days 29%; $\mathbf{L}^7$ 3 days 14.3%, 5 days 40%). It is likely that the low solubility of the resultant phenoxides, coupled with the enhanced reactivity of the dianions over the monoanions, is responsible for the sluggish dipropargylation. That is, the mono- and diphenoxides were both observed to be of low solubility, but it is likely that the dianionic species formed by double deprotonation of the starting material is highly reactive and is rapidly propargylated, either on the surface of the precipitate or by rapid exchange of the small quantity in solution. Upon monopropargylation, however, the remaining monoanionic species is apparently far less reactive and is still of low solubility, leading to a slow reaction. The syntheses of mono- and dialkynes based upon 1,5-dihydroxy anthraquinone ($\mathbf{L}^4$ and $\mathbf{L}^5$) were attempted; however, due to the poor yields obtained ($\mathbf{L}^4$, 4% and $\mathbf{L}^5$, 3%) under the conditions most suitable for the other isomers, this route was abandoned as impractical. The anions derived from 1,5-dihydroxyanthraquinone appeared to be the least soluble of all, and it is likely that the low yields merely reflect an extremely slow reaction. In all cases the conversion of the hydroxyanthraquinone to the desired alkynoxy products was initially indicated by the appearance of a signal in the ^{1}H NMR spectra characteristic of the methylene unit of the propargyl ether at 4.5−5.0 ppm with the characteristic propargyl coupling (d, $J_{HH} \approx 2.3$ Hz), which has shifted to higher frequency than the bromide starting material, along with the distinctive triplet ($J_{HH} \approx 2.3$ Hz) for the acetylenic proton at 2.0−2.5 ppm.

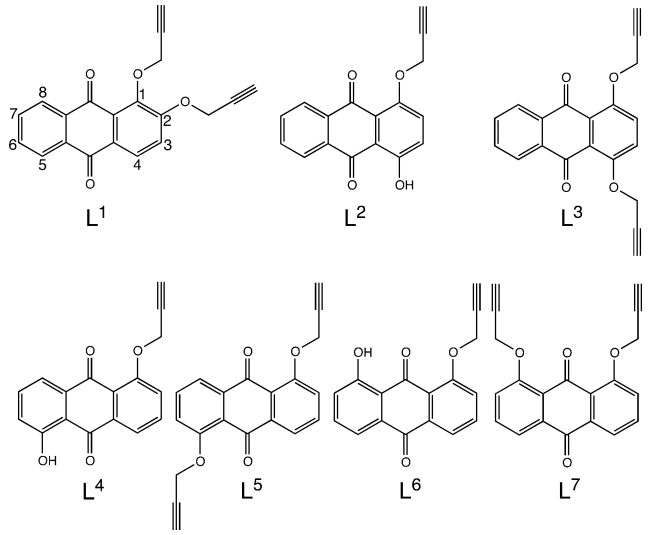

Figure 1. Key to structures of the ligands and (inset) gold complexes.

Synthesis of Complexes. With a series of mono- and dipropargylated dihydroxyanthraquinones available a study of their coordination chemistry with gold(I) was undertaken. Following a variation on standard procedures, each of the ligands was treated with a slight excess of the standard gold precursor [Cl-Au-PPh$_3$][21] in the dark, in the presence of potassium ethoxide, itself generated *in situ* from potassium *tert*-butoxide in ethanol. The monometallic products remained in solution and were easily isolated by filtration from the KCl

dx.doi.org/10.1021/om300475y | *Organometallics* 2012, 31, 5835−5843

byproduct and then evaporation; the dimetallic complexes precipitated from the reaction mixture and thus were isolated by filtration, redissolution in dichloromethane, refiltration, and evaporation of solvent. Each complex was purified by crystallization, using vapor diffusion of diethyl ether into a concentrated THF solution. It was observed that prolonged exposure to chlorinated solvents, especially chloroform, resulted in the breakdown of the complex and the recovery of the gold starting material [Cl-Au-PPh_3]. In each case formation of the desired product complexes was initially confirmed by ^{1}H NMR spectroscopy, in which disappearance of the acetylenic triplet (and a shift to higher frequency of the propargylic singlet) indicated terminal coordination of gold. $^{31}P\{^1H\}$ NMR spectra for the complexes also confirmed formation of a σ-bonded terminal Au(I) alkynyl triphenylphosphine species, with singlet resonances at around +42 ppm, in the region expected from literature precedent.[11] Mass spectrometry was not useful in these cases, as each of the complexes gave only a peak at 721 amu. This has been reported by Schmidbaur et al.[22] and observed previously by ourselves[23] and has been attributed to the ligand dissociation and then recombination to form $[Au(PPh_3)_2]^+$; attribution of this phenomenon was confirmed by a lack of a characteristic resonance for $[Au(PPh_3)_2]^+$ in the $^{31}P\{^1H\}$ NMR spectra.[24] Solid-state IR spectroscopy studies were also carried out, which showed subtle changes in the ν(CC) in comparison to the corresponding free ligands. The ligands display an IR stretching band typical of terminal aliphatic alkynes at 2120 cm^{-1}, whereas the complexes display a weaker intensity IR absorption band at around 2132 cm^{-1}.

Single-Crystal X-ray Diffraction Studies. Diffusion of diethyl ether into a concentrated chloroform solution, over a period of 24 h, of [L^7-(Au-PPh_3)$_2$] yielded pale orange crystals suitable for X-ray diffraction studies. The crystal solved in space group $P2_1/n$ and was refined using the SHELX suite of software to give confirmation of the structure of the expected molecule: two molecules of chloroform solvent per asymmetric unit enclosed within the crystal lattice (Figure 2).[25] Tables of bond angles and lengths are summarized in Table 1 (Supporting Information). The structure overall shows a nonplanar anthraquinone unit with the central ring distorted to give an open-book conformation (Figure 3) with an angle between the

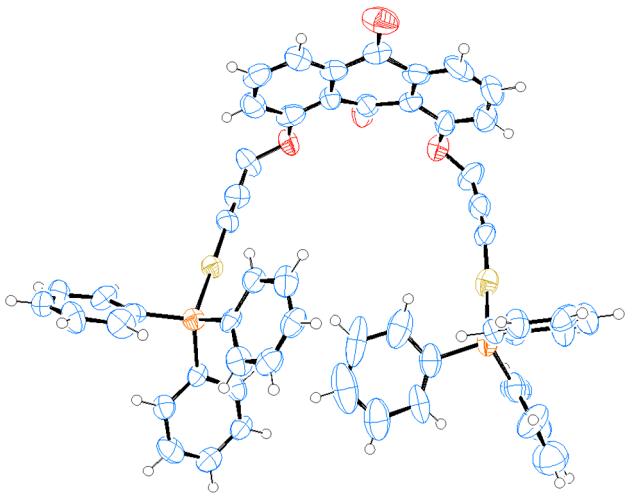

Figure 2. Molecular structure of [L^7-(Au-PPh_3)$_2$] (ORTEP,[26] 50% probability). Solvent molecules are omitted for clarity.

Table 1. Solution (MeCN, 10^{-5} M) Absorption and Emission (λ_{ex} = 345 nm) Data for the Ligands and Complexes

compound	absorption/nm	emission/nm
L^1	257, 369	398
[L^1-(Au-PPh_3)$_2$]	272, 375	406, 538, 566
L^2	270, 326, 432	408, 540 br
[L^2-Au-PPh_3]	272, 324 sh, 448	425, 522
L^3	268 sh, 302 sh, 394	487
[L^3-(Au-PPh_3)$_2$]	266 sh, 322 sh, 406	415, 435
L^7	254, 278 sh, 378	505
[L^7-(Au-PPh_3)$_2$]	257, 275 sh, 382	491

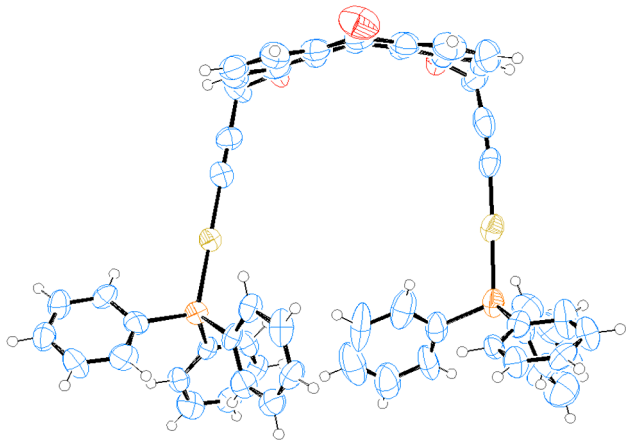

Figure 3. Molecular structure of [L^7-(Au-PPh_3)$_2$] (ORTEP,[26] 50% probability) showing curvature of the anthraquinone unit.

two terminal rings of approximately 161°. The two propargyloxy-gold-phosphine units are in a *cis* arrangement, overlapping one face of the anthraquinone, with the aromatic rings of the triphenyl phosphines proximate, but without any distinct close contacts indicating strong intramolecular π-stacking. However, examination of the packing of the asymmetric units reveals intramolecular close contacts (closer than the sum of the van der Waals radii) between adjacent molecules involving both the phenyl units of the phosphine ligands and the polarized anthraquinone rings. The *cis* arrangement therefore seems to be favored by the combination of weak intra- and stronger intermolecular π-stacking of the aromatic units of the phosphine ligands and, in particular, by facilitating the overlap of anthraquinone rings from adjacent molecules. The quinone oxygen *cis* to the propargyloxy units is distorted out of the plane of the C−C vector containing the two quinoid carbons, with a C−C−O angle of 155° (Figure 4). This oxygen is weakly hydrogen bonded (2.236 Å) to the hydrogen of a chloroform solvent of crystallization, but it is likely that the distortion is caused by electronic repulsion from the 1,8 dioxygens. The two-coordinate gold atoms are essentially linear, and the Au−C and Au−P distances lie within the range of literature values.[11]

UV−Vis Absorption and Luminescence Properties of the Ligands and Complexes. The UV−visible absorption properties of the ligands comprise IL π−π* (both aryl and alkynyl) transitions of <310 nm, with a broadened lowest energy contribution (Figure 5) expected to comprise significant charge transfer character arising from O(alkoxy)-to-quinone transitions,[27,28] with L^2 displaying the greatest bathochromic shift in the visible region. When compared to the relevant free

dx.doi.org/10.1021/om300475y | *Organometallics* 2012, 31, 5835−5843

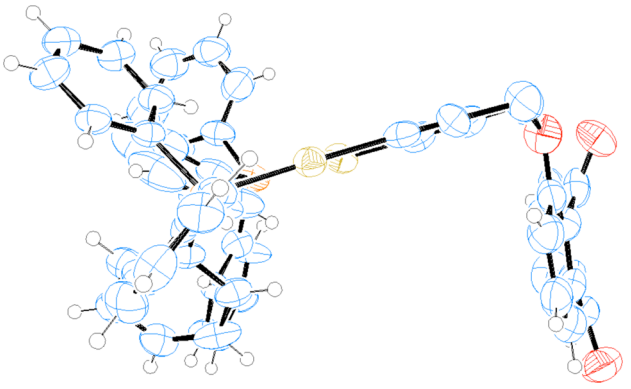

Figure 4. Molecular structure of [L^7-(Au-PPh_3)$_2$] (ORTEP,[26] 50% probability) showing distortion of the quinoid oxygens.

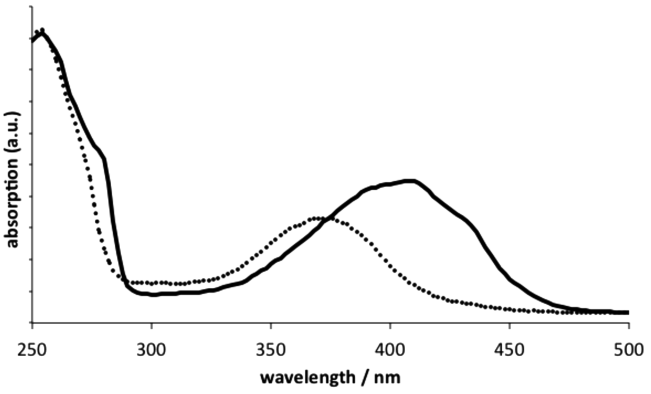

Figure 5. UV−vis absorption (MeCN) spectra comparing L^6 (solid line) and L^7 (dashed line).

ligands, the absorption spectra of the complexes principally reveal increased absorption coefficients, <270 nm, corresponding to the presence of multiple phenyl chromophores (associated with the "Au-PPh_3" units). Of course, Au-alkynyl species have been shown to possess metal-to-alkynyl charge transfer (MLCT) bands, and these are presumed to contribute to the overlapping spectral profile at 300−400 nm.[29] However, the broad, unstructured visible absorption characteristics of the complexes can be wholly attributed to the appended anthraquinone chromophores in each case; very minor shifts are noted for these bands upon coordination of Au(I) to the alkyne termini. It is also noteworthy that within this series the 1,4-disubstituted anthraquinone species L^2 and [L^2-Au-PPh_3] possessed the largest bathochromic shift for the charge transfer band.

In terms of the luminescence properties, the visible emission spectra (λ_{ex} = 340−400 nm; aerated MeCN) for these anthraquinone species are quite broad in appearance, with some examples (e.g., L^3) revealing poorly resolved vibronic features. The broadness of the emission profiles is again consistent with a charge transfer dominated excited state,[27,30,31] and this assignment, together with the emission energies, compares quite well to the visible emission characteristics shown by related parent hydroxy-anthraquinones. In accordance with related work on amino- and alkoxy-substituted anthraquinones,[16,29,30] the emission properties of this series of alkoxy derivatives also show pronounced variations according to substituent position. The emission from the 1,2-anthraquinone is at the shortest wavelength, with the 1,4- and 1,8-disubstituted species with intermediate to lower relative energies. In this series, the comparison of L^1 with L^2 revealed an additional, lower energy emission peak at ca. 550 nm for the latter. The dual emissive nature of related dihydroxy-anthraquinone species[30,31] has been attributed to the tautomerized 1,10-keto form of the ligand (versus the 9,10-keto form); dual emission actually arises from the excited-state intramolecular proton transfer between the 4-hydroxy substituent and the neighboring carbonyl. However, the 1,10-keto form usually absorbs and emits at lower energy,[31] and therefore it may be that for L^2 (and [L^2-Au-PPh_3]) the higher energy emission peak at 409 nm is actually due to the 9,10-keto form and that tautomerization accounts for the dual emission.

The luminescence properties (λ_{ex} = 340−400 nm; aerated MeCN) of the complexes are again dictated by the nature of the appended anthraquinone chromophore (Table 1), with no clear evidence for long-lived $M_{Au}L_{alkyne}CT$ phosphorescence. The spectra showed that for dual-emissive [L^2-Au-PPh_3], the relative intensities of the peaks were sensitive to the complexation of Au(I) and the nature of the solvent.[28,29] Nonpolar solvents ($CHCl_3$) promote the long-wavelength form, whereas in polar protic solvent the emission profile was dominated by the shorter wavelength fluorescence. The emission behavior of this type of anthraquinone chromophore is notoriously sensitive to solvent,[31,32] and H-bonding can provide very effective pathways for excited-state quenching.[27] The emission profile of [L^3-(Au-PPh_3)$_2$] was unusually broad and ill-defined, with a lowest energy maximum at 524 nm. In contrast, the spectral profile for [L^7-(Au-PPh_3)$_2$] showed a single emission peak at 491 nm (Figure 6), which was subtly

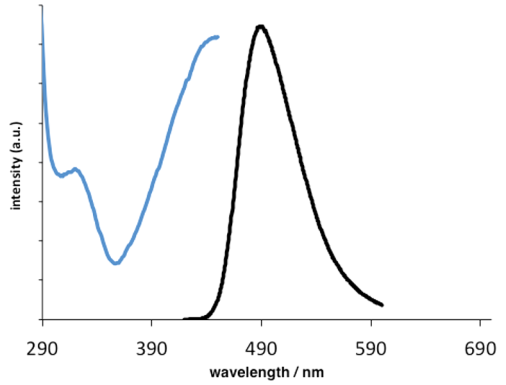

Figure 6. Excitation (left) and emission (right) spectra for [L^7-(Au-PPh_3)$_2$].

hypsochromically shifted relative to the free ligand, L^7. It is worth considering the severe out-of-plane distortion revealed by the solid-state structure of [L^7-(Au-PPh_3)$_2$]: such a distortion would be expected to perturb the energetics of the O(alkoxy)-to-quinone charge transfer excited state. Time-resolved measurements revealed that the luminescence lifetimes associated with the ligands are comparable to previous reports relating to donor-functionalized anthraquinone chromophores:[31] the emission was short-lived (<5 ns) and indicative of fluorescence in all cases. For the complexes, the lifetimes are also similarly short, which is again attributed to the fluorescence of the anthraquinone chromophore; there was no evidence for heavy atom assisted phosphorescence from the complexes.

Cytotoxicity Studies. A preliminary study of the cytotoxicity of some selected ligands (L^2, L^3, and L^7) and the

dx.doi.org/10.1021/om300475y | *Organometallics* 2012, 31, 5835−5843

corresponding complexes ([L^2-Au-PPh_3], [L^3-(Au-PPh_3)$_2$], and [L^7-(Au-PPh_3)$_2$]) was undertaken using the MTT assay with four different cancer cell lines: MCF7 (breast adenocarcinoma), A549 (lung adenocarcinoma), PC3 (prostate adenocarcinoma), and LOVO (colon adenocarcinoma). For the MTT assay, the compounds were initially dissolved in DMSO, and doses of 0.1, 1, 10, and 100 μM were tested to analyze the activity of different concentrations and then compared to a control medium with no treatment. The approximate IC_{50} values for these compounds are shown in Table 2.

Table 2. Cytotoxicity of Ligands and Complexes[a]

ligand/complex	IC_{50} MCF7	IC_{50} PC3	IC_{50} A549	IC_{50} Lovo
L^2	80	>100	>100	>100
[L^2-Au-PPh_3]	5	50	100	100
L^3	>100	>100	>100	70
[L^3-(Au-PPh_3)$_2$]	5	50	>100	80
L^7	>100	>100	>100	>100
[L^7-(Au-PPh_3)$_2$]	5	>100	>100	>100

[a]MTT assay: full experimental details are provided in the Supporting Information.

It is clear from the data presented in Table 2 that the gold(I) complexes are dramatically more toxic than the corresponding free ligands, which is gratifying, as it demonstrates that the observed cytotoxicity is a result of the chemistry associated with the gold alkynyl unit, rather than the biological properties of the anthraquinones. Thus, the anthraquinone, which is useful in this context for both luminescence and the potential to direct the localization of the complexes in cells, has not dominated the cellular behavior. Also obvious was that all of the complexes were considerably more cytotoxic to MCF7s than the other cell lines tested, although the cytotoxicities are not in themselves particularly low, even in MCF7s (cf. [AuCl(PPh_3)][33] $IC_{50} \approx 2.6$ and cisplatin IC_{50} = 2.0 μM). It is noteworthy that the complexes show much greater toxicity in MCF7s, a cell line known to have a higher mitochondrial mass than many other immortal cell lines, which are often deficient in mitochondrial activity in line with the "Warburg effect",[34] given that the mitochondria are believed to be the key intracellular target of gold agents.[5] Interestingly, this series of complexes appear to be much less cytotoxic than related Au(I) tertiary phosphine species incorporating biologically inspired mercapto-pteridine ligands.[35] Having established that the complexes displayed toxicity toward MCF7s, and in light of earlier imaging studies that indicated lysosomal entrapment for some gold agents, attention subsequently turned to the study of cellular distribution by fluorescence microscopy.

Live Cell Imaging Studies. Having established the photophysical properties of ligands and complexes and undertaken a study of their cytotoxicity in a variety of cell lines, their cellular uptake and localization in MCF-7 cells (one of the cell lines used in the toxicity study that had shown the most sensitivity to the complexes) was investigated. For the imaging studies the dialkynyl ligand, L^3, and examples of both mono- and dimetallic gold complexes, [L^2-Au-PPh_3] and [L^3-(Au-PPh_3)$_2$], were selected for investigation, as these had shown promising cytotoxicity and/or were of interest as a ligand−complex comparison. The incubations were carried out at 4 °C, at which temperature energy-dependent uptake processes, such as endocytosis, are inhibited in order to avoid entrainment in endosomes and in order to allow a comparison of the intrinsic membrane permeancy of the species. The cells were washed free of excess agent, then allowed to warm to ambient temperature to allow energy-dependent intracellular distribution pathways to re-emerge, while blocking energy-dependent uptake, before examination by confocal laser microscopy. In all cases the excitation wavelength was 405 nm and the images were collected between 530 and 580 nm, correlating to the low-energy tail of the anthraquinone emission, and thus well separated from endogenous autofluorescence. The dialkynyl ligand L^3 showed (Figure 7) good

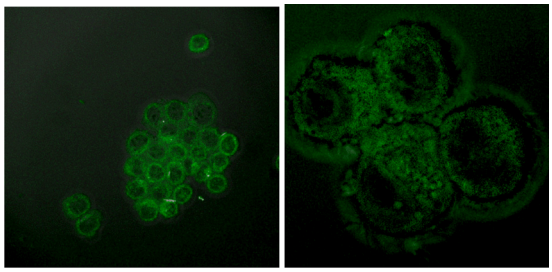

Figure 7. Images of MCF-7 cells incubated with L^3 (100 μg mL^{-1}, 4 °C, 30 min). Excited at 405 nm, acquired 530−580 nm.

uptake, with >80% of the population showing fluorophore-based emission and possessing a healthy cell morphology. The emission was reasonable, although not particularly bright, and was detected throughout the cytoplasm, with little or no nuclear localization. Although there appeared to be certain "hot spots" of luminescence in individual cells, the localization was clearly not specific to a particular organelle, but was throughout a variety of cytoplasmic structures.

The monogold complex [L^2-Au-PPh_3] was again taken up by >80% of the cell population, and again apparently healthy cell morphology was retained (Figure 8). In this case the

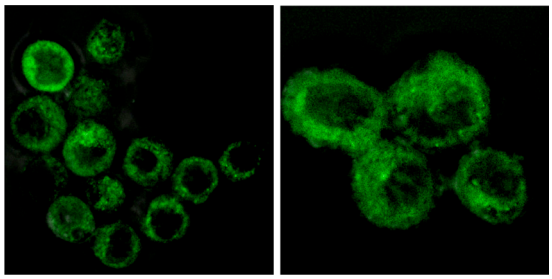

Figure 8. Images of MCF-7 cells incubated with [L^2-Au-PPh_3] (100 μg mL^{-1}, 4 °C, 30 min). Excited at 405 nm, acquired 530−580 nm.

luminescence was considerably increased, which is likely to indicate better uptake as a result of the enhanced lipophilicity of [L^2-Au-PPh_3] compared to L^2 upon inclusion of the triphenyl phosphine units. Again the luminescence originated from the cytoplasm, with little or no nuclear localization, and with certain bright spots indicating concentrations in certain organelles. Although these bright spots were more distinct than for the free ligand, the pattern of distribution may favor certain organelles. [L^2-Au-PPh_3] had clearly accumulated a significant concentration across the entire cytoplasm, including all organelles, which constitutes a significant proportion of the volume of the cytoplasm.

The dimetallic gold complex [L^3-(Au-PPh_3)$_2$] showed (as qualitatively judged by luminescence intensity) a similar uptake

dx.doi.org/10.1021/om300475y | Organometallics 2012, 31, 5835−5843

to the mononuclear complex [L^2-Au-PPh_3], which was unexpected from the additional lipophilicity of an additional triphenyl phosphine unit. The pattern of distribution (Figure 9)

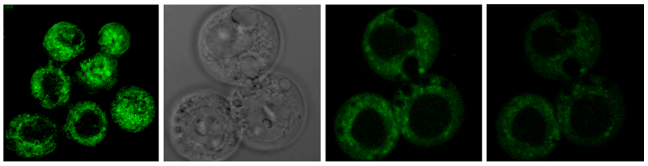

Figure 9. Images of MCF-7 cells incubated with [L^3-$(Au\text{-}PPh_3)_2$] (100 μg mL^{-1}, 4 °C, 30 min), excited at 405 nm, acquired 530−580 nm showing: (A) cytoplasmic distribution (overlaid luminescence and transmitted light); (B) appearance of vacuoles upon irradiation (transmitted light only); (C and D) photobleaching (luminescence only).

was also similar, with general cytoplasmic staining being apparent, with little or no nuclear localization, and with bright spots. It is possible that the sheer steric bulk of the complex impedes uptake by passive diffusion in line with Fick's law. However, intensity may be misleading in this case, due to photobleaching (see additional comment below). It was notable that, in addition to more severe photobleaching than was observed with L^2 and monomeric complex [L^2-Au-PPh_3], the cells showed apparent toxic effects upon irradiation, with large vacuoles appearing in the cells, which characterize membrane damage. It is possible that the phenomena of photobleaching and cell damage are linked, as photobleaching usually involves the generation of toxic species (e.g., oxygen radicals) through the reaction of the lumophore excited state with material in the environment. The unusually broad emission maximum of this complex, noted above, may indicate properties of the excited state that render photochemical reaction with the medium, and thus the generation of toxic species, more rapid than with the other complexes/ligands. While it is noted that this complex showed the broadest range of activity and lowest IC_{50} in the cytotoxicity studies described above, it should also be noted that at the outset of the imaging experiment the cells treated with [L^3-$(Au\text{-}PPh_3)_2$] appeared healthy (the time scales of the experiments are different) and the vacuoles appeared only upon irradiation, so while it is possible that the cytotoxicity and apparent phototoxicity are linked, this cannot be assumed.

CONCLUSIONS

The ligands L^{1-3} and $L^{6,7}$, which were prepared in useful quantity by functionalizing various hydroxyanthraquinone derivatives with propargylic groups, revealed luminescence properties attributable to the various isomeric forms of the substituted anthraquinone chromophoric cores. Upon formation of the gold complexes, changes in the emission profiles are observed, but there is no indication of triplet emission as a result of incorporating the heavy atom. It appears that the dominant features of the emission spectra are, in all cases, attributable to the anthraquinone-based processes, rather than transitions involving substantial metal character. The ligands generally show low cytotoxicity, while in all cases the complexes are considerably more toxic to one of the cell lines at least (MCF-7) and in some cases to more of the lines, indicative of a gold-dependent cytotoxicity. Cellular imaging utilizing the anthraquinone-based fluorescence showed that the agents are able to access organelles within the cytoplasm, in line with the suggested mode of gold cytotoxicity that involves mitochondrial inhibition.

EXPERIMENTAL SECTION

Cytotoxicity Assessment via MTT Assay. The cytotoxicity of the complexes was assessed using the colorimetic and quantitative MTT [3-(4,5-dimethylthiazol-2-yl)-2,5-diphenyltetrazolium bromide] assay, first reported by Mosmann et al.[36] Quantification was achieved using a multiwell scanning spectrophotometer and is reported as an IC_{50} value.[33]

Method for Cytotoxicity Analysis. Antitumor evaluation in MCF7, LoVo, A549, and PC3 cell lines was performed by the MTT assay. Compounds were prepared as 0.1−100 mM stock solutions dissolved in DMSO and stored at −20 °C. Cells were seeded into 96-well microtiter plates at a density of 5×10^3 cells per well and allowed 24 h to adhere. Decimal compound dilutions were prepared in medium immediately prior to each assay (final concentration 0.1−100 μM). Experimental medium was DMEM + 10% FCS (PC3 and Lovo) or RPMI + 10% heat-inactivated FCS (A549 and MCF7). Following 96 h compound exposure at 37 °C and 5% CO_2, MTT reagent (Sigma Aldrich) was added to each well (final concentration 0.5 mg/mL). Incubation at 37 °C for 4 h allowed reduction of MTT by viable cells to an insoluble formazan product. MTT was removed and formazan solubilized by addition of 10% Triton X-100 in phosphate buffer saline (PBS). Absorbance was read on a Tecan Sunrise spectrophotometer at 540 nm as a measure of cell viability; thus inhibition relative to control was determined (IC_{50}).

Human Cell Incubation and Confocal Microscopy. Human adenocarcinoma cells (MCF-7), obtained from the European Collection of Cell Cultures (Porton Down, Wiltshire, UK), were maintained in Hepes modified minimum essential medium supplemented with 10% fetal bovine serum, penicillin, and streptomycin. Cells were detached from the plastic flask using trypsin-EDTA solution and suspended in an excess volume of growth medium. The homogeneous cell suspension was then distributed into 1 mL aliquots, with each aliquot being subjected to incubation with a different lumophore. Lumophores were initially dissolved in DMSO (5 mg/mL) before being added to the cell suspensions (final concentration 100 μg mL^{-1}) before incubation at 4 °C for 30 min. Cells were finally washed three times in PBS (pH 7.2), removing lumophore from the medium, then harvested by centrifugation (5 min, 800g) and mounted on a slide for imaging. Preparations were viewed using a Leica TCS SP2 AOBS confocal laser microscope using a 63× or 100× objective, with excitation at 405 nm and detection at 530−580 nm.

Data Collection and Processing. Diffraction data for [L^7-$(Au\text{-}PPh_3)_2$] were collected on a Bruker-Nonius diffractometer equipped with a KappaCCD detector (Mo Kα radiation, λ = 0.71075 Å) from fine-focus sealed tube source equipped with a graphite monochromator at 100 K. Data collection was performed using COLLECT (Nonius BV, 1997−2001) with cell refinement and data reduction using Denzo/Scalepack.

Structure Analysis and Refinement. The structure was solved by direct methods using SHELXS-97[25] and was completed by iterative cycles of ΔF-syntheses and full-matrix least-squares refinement. All non-H atoms were refined anisotropically, and difference Fourier syntheses were employed in positioning idealized hydrogen atoms, which were allowed to ride on their parent C atoms. Disordered solvent molecules were modeled using partial occupancy. All refinements were against F^2 and used SHELXL-97. Figures were created using the ORTEP3 software package.[26]

Crystal data for [L^7-$(Au\text{-}PPh_3)_2$]: $C_{58}H_{38}Au_2Cl_6O_4P_2$, M = 1467.46, yellow plate, 0.35 × 0.30 × 0.04 mm^3, monoclinic, space group $P2_1/n$ (No. 14), a = 18.4561(9) Å, b = 11.6603(5) Å, c = 26.6072(7) Å, β = 98.614(2)°, V = 5661.4(4) $Å^3$, Z = 4, D_c = 1.722 g/cm^3, F_{000} = 2832, KappaCCD, Mo Kα radiation, λ = 0.71073 Å, T = 293(2) K, $2\theta_{max}$ = 55.1°, 12 698 reflections collected, 12 698 unique (R_{int} = 0.0000). Final GooF = 1.021, R_1 = 0.0871, wR_2 = 0.2013, R indices based on 6193 reflections with $I > 2(I)$ (refinement on F^2), 686 parameters, 63

dx.doi.org/10.1021/om300475y | Organometallics 2012, 31, 5835−5843

restraints. *Lp* and absorption corrections were applied; μ = 5.561 mm^{-1}.

All reactions were performed with the use of vacuum line and Schlenk techniques. Reagents were commercial grade and were used without further purification. ^1H and $^{13}C\{^1H\}$ NMR spectra were recorded on an NMR-FT Bruker 400 MHz or Joel Eclipse 300 MHz spectrometer and recorded in $CDCl_3$. ^1H and $^{13}C\{^1H\}$ NMR chemical shifts (δ) were determined relative to residual solvent peaks with digital locking; $^{31}P\{^1H\}$ chemical shifts (δ) were determined relative to H_3PO_4 and are given in ppm. Low-resolution mass spectra were obtained by the staff at Cardiff University. High-resolution mass spectra were carried out at the EPSRC National Mass Spectrometry Service at Swansea University. UV−vis studies were performed on a Jasco V-570 spectrophotometer as MeCN solutions (1×10^{-5} M). Photophysical data were obtained on a JobinYvon−Horiba Fluorolog spectrometer fitted with a JY TBX picosecond photodetection module as MeCN solutions. Emission spectra were uncorrected, and excitation spectra were instrument corrected. The pulsed source was a Nano-LED configured for 372 nm output operating at either 500 kHz or 1 MHz. Luminescence lifetime profiles were obtained using the JobinYvon−Horiba FluoroHub single photon counting module, and the data fits yielded the lifetime values using the provided DAS6 deconvolution software.

Synthesis of Ligands. *Synthesis of* L^1. To an excess of K_2CO_3 in acetone (40 mL) were added alizarin (0.500 g, 2.08 mmol) and propargyl bromide (0.320 mL, 4.37 mmol). The reaction mixture was heated at reflux for three days and then filtered. The filtrate was concentrated under reduced pressure to yield a light brown solid (yield: 0.260 g, 29%). ^1H NMR ($CDCl_3$, 400 MHz, 298 K): δ_H 2.48−2.53 (1H, m, C*H*), 2.58−2.62 (1H, m, C*H*), 4.84−4.96 (4H, m, CH_2), 7.42 (1H, d, $^3J_{HH}$ = 6.1 Hz, Ar*H*), 7.73−7.85 (2H, m, Ar*H*), 8.18−8.30 (3H, m, Ar*H*) ppm. $^{13}C\{^1H\}$ NMR ($CDCl_3$, 101 MHz, 298 K): δ_C 56.9, 61.0, 75.2, 77.2, 118.0, 118.4, 125.6, 126.8, 127.4, 127.9, 128.2, 132.9, 133.7, 133.8, 134.1, 135.0, 147.3, 157.1, 182.3, 182.6 ppm. MS (ES^+) *m*/*z*: 316.01 $[M + H]^+$. HR MS (ES^+): found *m*/*z* 317.0812; $[C_{20}H_{13}O_4]^+$ requires 317.0808. IR (Nujol) ν: 2129 (CC), 1673 (CO), 1568 (CO) cm^{-1}. UV−vis (ε/M^{-1} cm^{-1}) (MeCN) λ_{max}: 257 (47 000), 369 (11 000) nm.

Synthesis of L^2. The reaction was performed as for L^1, except using 1,4-dihydroxyanthraquinone (0.500 g, 2.08 mmol). Column chromatography (silica; CH_2Cl_2) was used to remove the dialkylated byproduct, and the desired monoalkylated product was isolated as an orange solid (yield: 0.085 g, 15%). ^1H NMR ($CDCl_3$, 400 MHz, 298 K): δ_H 2.49 (1H, t, $^3J_{HH}$ = 2.4 Hz, C*H*), 4.73 (2H, d, $^3J_{HH}$ = 2.4 Hz, CH_2), 7.12−7.16 (1H, m, Ar*H*), 7.37−7.41 (1H, m, Ar*H*), 7.63−7.81 (2H, m, Ar*H*), 8.13−8.24 (2H, m, Ar*H*) ppm. $^{13}C\{^1H\}$ NMR ($CDCl_3$, 101 MHz, 298 K): δ_C 58.4, 77.8, 115.5, 121.5, 126.1, 126.5, 126.5, 127.5, 128.1, 128.2, 133.6, 134.9, 135.0, 151.8, 158.7, 181.8, 188.9 ppm. ES MS *m*/*z*: 278 $[M]^+$, 240 $[M - C_3H_2]^+$. HR MS (ES^+): found *m*/*z* 278.0574; $[C_{17}H_{10}O_4]^+$ requires 278.0574. IR (Nujol) ν: 2115 (CC), 1666 (CO), 1663 (CO), 1593 (CO) cm^{-1}. UV−vis (ε/M^{-1} cm^{-1}) (MeCN) λ_{max}: 270 (27 000), 326 (5500), 432 (14 000) nm.

Synthesis of L^3. The reaction was performed as for L^2, but the reaction mixture was heated at reflux for five days to produce the dialkylated product. The filtrate was concentrated under reduced pressure to yield an orange solid (yield: 0.205 g, 23%). ^1H NMR ($CDCl_3$, 400 MHz, 298 K): δ_H 2.52 (2H, t, $^3J_{HH}$ = 2.4 Hz, C*H*), 4.79 (4H, d, $^3J_{HH}$ = 2.4 Hz, CH_2), 7.41 (2H, s, Ar*H*), 7.59−7.62 (2H, m, Ar*H*), 8.06−8.12 (2H, m, Ar*H*) ppm. $^{13}C\{^1H\}$ NMR ($CDCl_3$, 101 MHz, 298 K): δ_C 58.3, 77.4, 123.8, 126.6, 133.6, 155.8 (CO not observed) ppm. ES MS *m*/*z*: 316 $[M]^+$ 277.05 $[M - C_3H_3]^+$. HR MS (ES^+): found *m*/*z* 316.0746; $[C_{20}H_{12}O_4]^+$ requires 316.0730. IR (Nujol) ν: 2119 (CC), 1671 (CO), 1582 (CO) cm^{-1}. UV−vis (ε/M^{-1} cm^{-1}) (MeCN) λ_{max}: 275 (26 500), 302 (12 000), 394 (10 000) nm.

Synthesis of L^4. The reaction was performed as for L^1, except using 1,5-dihydroxyanthraquinone (0.500 g, 2.08 mmol). Column chromatography was used to isolate the monoalkylated species as an orange solid (yield: 0.025 g, 4%). ^1H NMR ($CDCl_3$, 400 MHz, 298 K): δ_H 2.52−2.60 (1H, m, C*H*), 4.89−4.95 (2H, m, CH_2), 7.21−7.28 (1H, m, Ar*H*), 7.48−7.52 (1H, m, Ar*H*), 7.62−7.70 (1H, m, Ar*H*), 7.7−7.82 (2H, m, Ar*H*), 7.98−8.05 (1H, m, Ar*H*) ppm. $^{13}C\{^1H\}$ NMR ($CDCl_3$, 101 MHz, 298 K): δ_C 57.3, 77.6, 119.0, 121.2, 121.8, 123.5, 132.9, 135.8, 138.1, 163.4 (CO not observed) ppm. ES MS *m*/*z*: 239.21 $[M - C_3H_3]^+$. HR MS (ES^+): found *m*/*z* 279.0652; $[C_{17}H_{11}O_4]^+$ requires 279.0652. IR (Nujol) ν: 2112 (CC), 1664 (CO), 1634 (CO), 1583 (CO) cm^{-1}. UV−vis (ε/M^{-1} cm^{-1}) (MeCN) λ_{max}: 254 (24 300), 408 (12 000) nm.

Synthesis of L^5. The reaction was performed as for L^4, but the reaction mixture was heated at reflux for three days with an extra portion of potassium carbonate in an attempt to produce the dialkylated species. The filtrate was concentrated under reduced pressure to yield an orange solid (yield: 0.012 g, 22%). ^1H NMR ($CDCl_3$, 400 MHz, 298 K): δ_H 2.48 (2H, t, $^3J_{HH}$ = 2.3 Hz, C*H*), 4.82 (4H, d, $^3J_{HH}$ = 2.3 Hz, CH_2), 7.37 (2H, d, $^3J_{HH}$ = 8.4 Hz, Ar*H*), 7.61−7.67 (2H, Ar*H*), 7.91 (2H, d, $^3J_{HH}$ = 7.7 Hz, Ar*H*) ppm.

Synthesis of L^6. The reaction was performed as for L^1 except using 1,8-dihydroxyanthraquinone (0.500 g, 2.08 mmol). Column chromatography was used to isolate the monoalkylated product as an orange solid (yield: 0.078 g, 13%). ^1H NMR ($CDCl_3$, 400 MHz, 298 K): δ_H 2.52 (1H, t, $^3J_{HH}$ = 2.36 Hz, C*H*), 4.91 (2H, d, $^3J_{HH}$ = 2.36 Hz, CH_2), 7.2 (1H, d, $^3J_{HH}$ = 9.43 Hz, Ar*H*), 7.42 (1H, d, $^3J_{HH}$ = 9.3 Hz, Ar*H*), 7.49−7.54 (1H, m, Ar*H*), 7.57−7.65 (2H, m, Ar*H*), 7.94 (1H, d, $^3J_{HH}$ = 8.7 Hz, Ar*H*) ppm. $^{13}C\{^1H\}$ NMR ($CDCl_3$, 101 MHz, 298 K): δ_C 57.2, 77.3, 118.9, 120.5, 121.2, 124.8, 135.8, 138.1, 161.0, 163.9 (CO not observed) ppm. MS (ES) *m*/*z*: 252 $[M - C_2H_3]^+$. HR MS (ES^+): found *m*/*z* 279.0651; $[C_{17}H_{10}O_4]^+$ requires 279.0652. IR (Nujol) ν: 2034 (CC), 1675 (CO), 1643 (CO), 1584 (CO) cm^{-1}. UV−vis (ε/M^{-1} cm^{-1}) (MeCN) λ_{max}: 254 (24 300), 408 (12 000) nm.

Synthesis of L^7. The reaction was performed as for L^6, but the reaction mixture was heated at reflux for five days to produce the dialkylated product. The filtrate was concentrated under reduced pressure to yield an orange solid (yield: 0.354 g, 40%). ^1H NMR ($CDCl_3$, 400 MHz, 298 K): δ_H 2.52 (2H, t, $^3J_{HH}$ = 2.34 Hz, C*H*), 4.88 (4H, d, $^3J_{HH}$ = 2.35 Hz, CH_2), 7.42 (2H, d, $^3J_{HH}$ = 8.3 Hz, Ar*H*), 7.51 (2H, app. t, $^3J_{HH}$ = 8.0 Hz, Ar*H*), 7.82 (2H, d, $^3J_{HH}$ = 7.8 Hz, Ar*H*) ppm. $^{13}C\{^1H\}$ NMR ($CDCl_3$, 101 MHz, 298 K): δ_C 57.3, 77.5, 120.4, 121.1, 133.8, 134.5, 157.2 (CO not observed) ppm. MS (ES) *m*/*z*: 277.04 $[M - C_3H_3]^+$. HR MS (ES^+): found *m*/*z* 316.0707; $[C_{20}H_{12}O_4]^+$ requires 316.0730. IR (Nujol) ν: 2130 (CC), 1671 (CO), 1658 (CO), 1585 (CO) cm^{-1}. UV−vis (ε/M^{-1} cm^{-1}) (MeCN) λ_{max}: 254 (29 200), 374 (10 400) nm.

Synthesis of Complexes. *Synthesis of* [L^1-(Au-PPh_3)$_2$]. To a round-bottom flask wrapped in Al foil were added L^1 (0.022 g, 0.07 mmol), [Cl-Au-PPh_3] (0.072 g, 0.15 mmol), and KO^{t}Bu (0.011 g, 0.1 mmol) in ethanol (2 mL), and the mixture was stirred under nitrogen for 12 h. The solution was concentrated, redissolved in chloroform, and filtered. The filtrate was concentrated *in vacuo* to produce a yellow solid (yield: 0.043 g, 48%). ^1H NMR ($CDCl_3$, 400 MHz, 298 K): δ_H 4.99−5.07 (4H, overlapping m, 2 × CH_2), 7.31−7.58 (32H, m, Ar*H*), 7.61−7.66 (1H, m, Ar*H*), 8.11−8.31 (3H, m, Ar*H*) ppm. $^{31}P\{^1H\}$ NMR ($CDCl_3$, 202.4 MHz, 298 K): δ_P +42.46 ppm. MS (ES^+) *m*/*z*: 721.15 $[Au(PPh_3)_2]^+$. IR (Nujol) ν: 2184 (CC), 1720 (CO) cm^{-1}. UV−vis (ε/M^{-1} cm^{-1}) (MeCN) λ_{max}: 273 (55 000), 375 (14 000) nm.

Synthesis of [L^2-Au-PPh_3]. To a round-bottom flask wrapped in Al foil were added L^2 (0.020 g, 0.074 mmol), [Cl-Au-PPh_3] (0.040 g, 0.080 mmol), and KO^{t}Bu (0.009 g, 0.80 mmol) in ethanol (2 mL), and the mixture was stirred under nitrogen for 12 h. Workup was like that for [L^1-(Au-PPh_3)$_2$] (yield: 0.015 g, 28%). ^1H NMR ($CDCl_3$, 400 MHz, 298 K): δ_H 5.01 (2H, s, CH_2), 7.16−7.23 (2H, m, Ar*H*), 7.3−7.42 (15H, m, Ar*H*), 7.62−7.79 (2H, m, Ar*H*) 8.12−8.19 (2H, m, Ar*H*) ppm. $^{31}P\{^1H\}$ NMR ($CDCl_3$, 202.4 MHz, 298 K): δ_P +42.4 ppm. MS (ES^+) *m*/*z*: 721.15 $[Au(PPh_3)_2]^+$. IR (Nujol) ν: 2133 (CC), 1665 (CO), 1664 (CO), 1593 (CO) cm^{-1}. UV−vis (ε/M^{-1} cm^{-1}) (MeCN) λ_{max}: 272 (24 400), 448 (10 600) nm. Anal. Calcd (%) for $AuPC_{35}H_{24}O_4(MeCN)(H_2O)_4$: C, 52.31; H, 4.15; N, 1.65. Found (%): C, 52.87; H, 4.05; N, 1.08.

Synthesis of [L^3-(Au-PPh_3)$_2$]. The reaction was performed as for [L^1-(Au-PPh_3)$_2$] except using L^3 (0.016 g, 0.101 mmol), giving the product as an orange solid (yield: 0.022 g, 36%). ^1H NMR ($CDCl_3$,

dx.doi.org/10.1021/om300475y | *Organometallics* 2012, 31, 5835−5843

400 MHz, 298 K): δ_H 5.01 (4H, s, CH_2), 7.23−7.45 (30H, m, Ar*H*), 7.48−7.53 (2H, m, Ar*H*), 7.68 (2H, s, Ar*H*), 8.01−8.20 (2H, m, Ar*H*) ppm. $^{31}P\{^1H\}$ NMR ($CDCl_3$, 202.4 MHz, 298 K): δ_P +42.46 ppm. MS (ES^+) *m*/*z*: 721.15 $[Au(PPh_3)_2]^+$. IR (Nujol) ν: 2021 (CC), 1898 (CO), 1666 (CO) cm^{-1}. UV−vis (ε/M^{-1} cm^{-1}) (MeCN) λ_{max}: 250 (12 700), 406 (1800) nm. Anal. Calcd (%) for $Au_2P_2O_4C_{56}H_{40}(H_2O)_{18}$: C, 43.20; H, 4.92. Found (%): C, 42.75; H, 4.11.

Synthesis of [L⁷-(Au-PPh₃)₂]. The reaction was performed as for $[L^1\text{-}(Au\text{-}PPh_3)_2]$ except using L^7 (0.010 g, 0.030 mmol), giving the product as an orange solid (yield: 0.032 g, 50%). ^1H NMR ($CDCl_3$, 300 MHz, 298 K): δ_H 5.08 (4H, s, CH_2), 7.33−7.52 (30H, m, Ar*H*), 7.63 (2H, app. t, $^3J_{HH}$ = 7.96 Hz, Ar*H*), 7.72−7.79 (2H, m, Ar*H*), 7.81−7.84 (2H, m, Ar*H*) ppm. $^{31}P\{^1H\}$ NMR ($CDCl_3$, 202.4 MHz, 298 K): δ_P +42.48 ppm. MS (ES^+) *m*/*z*: 721.29 $[Au(PPh_3)_2]^+$. IR (Nujol) ν: 2239 (CC), 2129 (CC), 1667 (CO), 1584 (CO) cm^{-1}. UV−vis (ε/M^{-1} cm^{-1}) (MeCN) λ_{max}: 257 (19 600), 397 (4700) nm.

■ ASSOCIATED CONTENT

Ⓢ Supporting Information

This material is available free of charge via the Internet at http://pubs.acs.org.

■ AUTHOR INFORMATION

Corresponding Author

*E-mail: cooganmp@cf.ac.uk; popesj@cardiff.ac.uk.

Notes

The authors declare no competing financial interest.

■ ACKNOWLEDGMENTS

We thank Cardiff University and EPSRC for financial support and the staff of the EPSRC Mass Spectrometry National Service (University of Swansea) for providing MS data.

■ REFERENCES

(1) Lewis, M. G.; DaFonseca, S.; Chomont, N.; Palamara, A. T.; Tardugno, M.; Mai, A.; Collins, M.; Wagner, W. L.; Yalley-Ogunro, J.; Greenhouse, J.; Chirullo, B.; Norelli, S.; Garaci, E.; Savarino, A. *AIDS* **2011**, *25*, 1347.

(2) (a) Parish, R. V.; Howe, B. P.; Wright, J. P.; Mack, J.; Pritchard, R. G.; Elsome, A. M.; Fricker, S. P. *Inorg. Chem.* **1996**, *35*, 1659. (b) Buckley, R. G.; Elsome, A. M.; Fricker, S. P.; Parish, R. V.; Howe, B. P.; Kelland, L. R. *J. Med. Chem.* **1996**, *39*, 5208.

(3) (a) Baker, M. V.; Barnard, P. J.; Berners-Price, S. J.; Brayshaw, S. K.; Hickey, J L.; Skelton, B. W.; White, A. H. *Dalton Trans.* **2006**, 3708. (b) Hickey, J. L.; Ruhayel, R. A.; Barnard, P. J.; Baker, M. V.; Berners-Price, S. J.; Filipovska, A. *J. Am. Chem. Soc.* **2008**, *130*, 12570.

(4) Chui, C.-H.; Wong, R. S.-M.; Gambari, R.; Cheng, G. Y.-M.; Yuen, M. C.-W.; Chan, K.-W.; Tong, S.-W.; Lau, F.-Y.; Lai, P. B.-S.; Lam, K.-H.; Ho, C.-L.; Kan, C.-W.; Leung, K. S.-Y.; Wong, W.-Y. *Bioorg. Med. Chem.* **2009**, *17*, 7872.

(5) (a) Berners-Price, S. J.; Filipovska, A. *Metallomics* **2011**, *3*, 863. (b) Ott, I. *Coord. Chem. Rev.* **2009**, *253*, 1670. (c) Barnard, P. J.; Berners-Price, S. J. *Coord. Chem. Rev.* **2007**, *251*, 1889. (d) McKeage, L. M.; Berners-Price, S. J. *Coord. Chem. Rev.* **2002**, *232*, 127. (e) Abdou, H. E.; Mohamed, A. A.; Fackler, J. P., Jr.; Burini, A.; Galassi, R.; Lopez-de-Luzuriaga, J. M.; Olmos, M. E. *Coord. Chem. Rev.* **2009**, *253*, 1661. (f) Bruijnincx, P. C. A.; Sadler, P. J. *Curr. Opin. Chem. Biol.* **2008**, *12*, 197.

(6) Williams, C. H., Jr. *Eur. J. Biochem.* **2000**, *267*, 6101.

(7) Barnard, P. J.; Wedlock, L. E.; Baker, M. V.; Price, S. J. B.; Joyce, D. A.; Skelton, B. W.; Steer, J. H. *Angew. Chem., Int. Ed.* **2006**, *45*, 5966.

(8) (a) Ott, I.; Qian, X.; Xu, Y.; Vlecken, D. H. W.; Marques, I. J.; Kubutat, D.; Will, J.; Sheldrick, W. S.; Jesse, P.; Prokop, A.; Bagowski, C. P. *J. Med. Chem.* **2009**, *52*, 763. (b) Ott, I.; Xu, Y. F.; Liu, J. W.; Kokoschka, M.; Harlos, M.; Sheldrick, W. S.; Qian, X. H. *Bioorg. Med. Chem.* **2008**, *16*, 7107. (c) Bagowski, C. P.; You, Y.; Scheffler, H.; Vlecken, D. H.; Schmitz, D. J.; Ott, I. *Dalton Trans.* **2009**, 10799.

(9) Vergara, E.; Cerrada, E.; Casini, A.; Zava, O.; Laguna, M.; Dyson, P. J. *Organometallics* **2010**, *29*, 2596.

(10) Evans, R. C.; Douglas, P.; Winscom, C. J. *Coord. Chem. Rev.* **2006**, *250*, 2093.

(11) (a) Yam, V. W.-W.; Lo, K. K.-W.; Wong, K. M.-C. *J. Organomet. Chem.* **1999**, *578*, 3. (b) Yam, V. W.-W.; Choi, S. W.-K. *J. Chem. Soc., Dalton Trans.* **1996**, 4227. (c) Ferrer, M.; Rodriguez, L.; Rosell, O.; Pina, F.; Lima, J. C.; Bardia, M. F.; Solans, X. *J. Organomet. Chem.* **2003**, *678*, 82. (d) Irwin, M. J.; Vittal, J. J.; Puddephatt, R. J. *Organometallics* **1997**, *16*, 3541. (e) Chao, H. Y.; Lu, W.; Li, Y. Q.; Chan, M. C.; Che, C. M.; Cheung, K. K.; Zhu, N. Y. *J. Am. Chem. Soc.* **2002**, *124*, 14696. (f) Vicente, J.; Gil-Rubio, J.; Barquero, N.; Jones, P. G.; Bautista, D. *Organometallics* **2008**, *27*, 646. (g) Riva, H.; Nieuwhuyzen, M.; Fierr, C. M.; Raithby, P. R.; Male, L.; Lagunas, M. C. *Inorg. Chem.* **2006**, *45*, 1418.

(12) (a) Kalyanraman, B.; Perez-Reyes, E.; Mason, R. P. *Biochim. Biophys. Acta* **1980**, *630*, 119. (b) Butler, J.; Hoey, B. M. *Biochim. Biophys. Acta* **1987**, *925*, 144.

(13) (a) Umadevi, M.; Vanelle, P.; Terme, T.; Rajkumar, J. M.; Ramakrishnan, V. *J. Fluoresc.* **2008**, *18*, 1139. (b) Tanaka, T.; Kohno, H.; Murakami, M.; Shimada, R.; Kagami, S. *Oncol. Rep.* **2000**, *7*, 501. (c) Shi, W.; Coleman, R. S.; Lowary, T. L. *Org. Biomol. Chem.* **2009**, *7*, 3709. (d) Eriksson, M.; Norden, B.; Eriksson, S. *Biochemistry* **1988**, *27*, 8144.

(14) Hou, Y.; Cao, S.; Brodie, P. J.; Callmander, M. W.; Ratovoson, F.; Rakotobe, E. A.; Rasamison, V. E.; Ratsimbason, M.; Alumasa, J. N.; Roepe, P. D.; Kingston, D. G. I. *Bioorg. Med. Chem.* **2009**, *17*, 2871.

(15) He, Z. H.; He, M. F.; Ma, S. C.; But, P. P. H. *J. Ethnopharmacol.* **2009**, *121*, 313.

(16) Jones, J. E.; Kariuki, B. M.; Ward, B. D.; Pope, S. J. A. *Dalton Trans.* **2011**, *40*, 3498.

(17) Jones, J. E.; Pope, S. J. A. *Dalton Trans.* **2009**, 8421.

(18) Jones, J. E.; Amoroso, A. J.; Dorin, I. M.; Parigi, G.; Ward, B. D.; Buurma, N. J.; Pope, S. J. A. *Chem. Commun.* **2011**, *47*, 3374.

(19) (a) Bryce, N. S.; Zhang, J. Z.; Whan, R. M.; Yamamoto, N.; Hambley, T. W. *Chem. Commun.* **2009**, 2673. (b) Alderden, R. A.; Mellor, H. R.; Modok, S.; Hall, M. D.; Sutton, S. R.; Newville, M. G.; Callaghan, R.; Hambley, T. W. *J. Am. Chem. Soc.* **2007**, *129*, 13400.

(20) Burchell, T. J.; Jennings, M. C.; Puddephatt, R. J. *Inorg. Chim. Acta* **2006**, *359*, 2812−2818.

(21) Braunstein, P.; Lehner, H.; Matt, D. *Inorg. Synth.* **1990**, *27*, 218.

(22) Thwaite, S. E.; Schier, A.; Schmidbaur, H. *Inorg. Chem.* **2004**, *357*, 1549.

(23) Mullice, L. A.; Thorp-Greenwood, F. L.; Laye, R. H.; Coogan, M. P.; Kariuki, B. M.; Pope, S. J. A. *Dalton Trans.* **2009**, 6836.

(24) Albano, V. G.; Busetto, L.; Cassani, M. C.; Sabatino, P.; Schmitz, A.; Zanotti, V. *J. Chem. Soc., Dalton Trans.* **1995**, 2087.

(25) Sheldrick, G. M. *Acta Crystallogr.* **2008**, *A64*, 112.

(26) Farrugia, L. J. *J. Appl. Crystallogr.* **1997**, *30*, 565.

(27) Diaz, A. N. *J. Photochem. Photobiol. A* **1990**, *53*, 141.

(28) (a) Yoshida, Z.; Takabayashi, F. *Tetrahedron* **1968**, *24*, 913. (b) Hongfeng, G.; Giesse, R.; Peters, A. T. *Dyes Pigments* **1996**, *31*, 323. (c) Reta, M. R.; Cattana, R.; Anunziata, J. D.; Silber, J. J. *Spectrochim. Acta* **1993**, *49A*, 903. (d) Perpete, E. A.; Wathelet, V.; Preat, J.; Lambert, C.; Jacquemin, D. *J. Chem. Theory Comput.* **2006**, *2*, 434.

(29) Yam, V. W. W.; Cheung, K. L.; Yip, S. K.; Cheung, K. K. *J. Organomet. Chem.* **2003**, *681*, 196.

(30) Umadevi, M.; Vanelle, P.; Terme, T.; Rajkumar, B. J. M.; Ramakrishnan, V. *J. Fluoresc.* **2008**, *18*, 1139. Richtol, H. H.; Fitch, B. R. *Anal. Chem.* **1974**, *46*, 1749.

(31) (a) Flom, S. R.; Barbara, P. F. *J. Phys. Chem.* **1985**, *89*, 4489. (b) Dahiya, P.; Kumbhakar, M.; Maity, D. K.; Mukherjee, T.; Mittal, J. P.; Tripathi, A. B. R.; Chattopadhyay, N.; Pal, H. *Photochem. Photobiol. Sci.* **2005**, *4*, 100. (c) Dahoya, P.; Kumbhakar, M.; Mukherjee, T.; Pal, H. *J. Mol. Struct.* **2006**, *798*, 40.

(32) Person, A. L.; Cornard, J.-P.; Say-Liang-Fat, S. *Chem. Phys. Lett.* **2011**, *517*, 41.
(33) Scheffler, H.; You, Y.; Ott, I. *Polyhedron* **2010**, *29*, 66.
(34) Yu, M. *Life Sci.* **2011**, *89*, 65.
(35) Mullice, L. A.; Mottram, H. J.; Hallett, A. J.; Pope, S. J. A. *Eur. J. Inorg. Chem.* **2012**, 3054.
(36) Mosmann, T. *J. Immunol. Methods* **1983**, *65*, 55.